Influence of Macro- and Microscopic Paper Structures on the Seam Strength in Ultrasonic Bonding of Fiber-based Materials

Nema Aldarwich,[a,*] Johannes Rauschnabel,[a] André Hofmann,[b] and Jens-Peter Majschak [b]

*Corresponding author: Nema.aldarwich@syntegon.com

DOI: 10.15376/biores.21.2.3593-3608

GRAPHICAL ABSTRACT

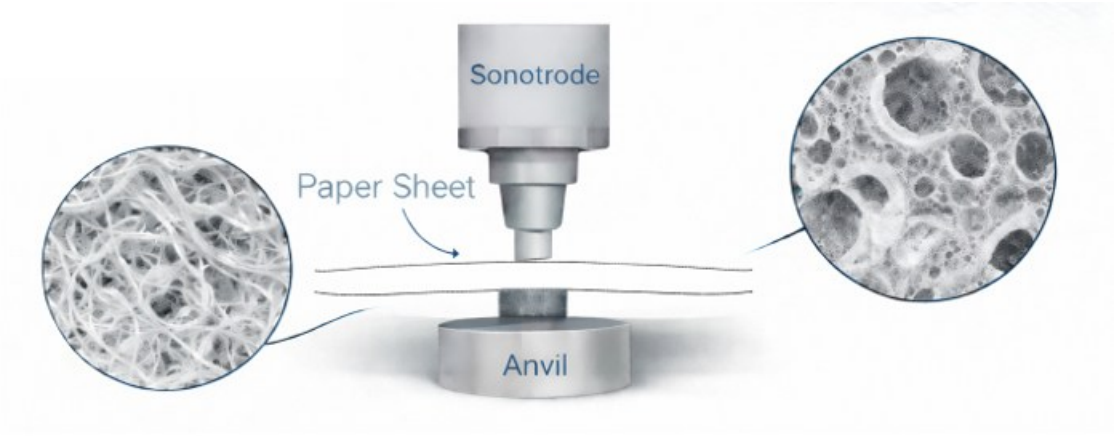

Influence of Macro- and Microscopic Paper Structures on the Seam Strength in Ultrasonic Bonding of Fiber-based Materials

Nema Aldarwich,[a,*] Johannes Rauschnabel,[a] André Hofmann,[b] and Jens-Peter Majschak [b]

The joint strength that develops in ultrasonic bonding of fiber-based materials is governed by multiple macro- and microscopic structural parameters whose interactions complicate the isolation of individual effects. In this study, paper made from cellulose-containing natural fibers was examined with respect to three structural factors: fiber orientation, paper side, and refining degree (°SR). Fiber orientation proved to be the dominant parameter. Samples with fibers aligned along the vibration direction exhibited significantly higher joint strengths than those with fibers oriented perpendicularly. The effect of paper side varied depending on fiber type and basis weight, indicating additional influences from factors such as porosity, surface roughness, and fiber distribution. Consequently, no universal relationship between paper side and joint strength was established. The refining degree showed no distinct influence within the typical range (°SR 24 to 36); however, at an exceptionally high value (°SR 80), a clear effect was observed. The impact of refining degree was found to depend strongly on basis weight: at 170 g/m², increased fibrillation enhanced bonding due to larger specific surface area, while at 80 g/m², shortened fibers and fewer contact points reduced joint strength. These findings highlight the need for a differentiated evaluation of structural parameters in optimizing ultrasonic bonding of fiber-based materials.

DOI: 10.15376/biores.21.2.3593-3608

Keywords: Paper; Fibrous materials; Joining; Sealing; Ultrasound

*Contact information: a: Syntegon Technology GmbH, Advanced Technology Development and Innovation, ETI, Stuttgarter Str. 130, D-71332 Waiblingen; b: TUD Dresden University of Technology, Fakultät Maschinenwesen 01062 Dresden; *Corresponding author: Nema.aldarwich@syntegon.com*

INTRODUCTION

The mechanical properties of paper are determined by a complex interplay of macroscopic and microscopic structural parameters. Key influencing factors include fiber orientation, the two-sidedness of the sheet, fiber length, and the degree of fiber fibrillation caused by refining. These factors not only affect the strength and stiffness of paper but also a variety of application-relevant functional properties such as printability, adhesive absorption, wettability, and coatability. In many cases, clear correlations between these structural features and performance in specific processing applications can be demonstrated. Against this background, it appears plausible that the same parameters that influence ink transfer or adhesion behavior also play a crucial role in the ultrasonic bonding of paper. An isolated consideration of individual structural features is insufficient to comprehensively describe the behavior of paper-based materials under bonding stress. Rather, an integrative analysis of micro- and macroscopic influencing factors is required

to accurately predict and optimize the resulting joint quality and strength.

Paper is an anisotropic fiber-reinforced material whose mechanical properties vary significantly with spatial direction. During sheet formation, cellulose fibers predominantly align in the machine direction (MD) as a result of flow-induced forces, while exhibiting substantially lower orientation in the cross direction (CD) and, in particular, in the thickness direction (ZD). This anisotropic structure results in properties such as tensile strength, stiffness, and water absorption being significantly higher in MD than in CD or ZD (Alava and Niskanen 2006). Findings from the field of fiber-reinforced thermoplastics suggest that fiber orientation in the joining zone directly influences joint quality. When the fiber orientation is parallel to the welding direction, it promotes more uniform energy input, controlled polymer flow, and a more homogeneous weld (Köhler *et al.* 2021). Transferring these insights to ultrasonic bonding of paper, it appears plausible that samples with fiber orientation parallel to the ultrasonic vibrations may also exhibit higher joint strength.

Another relevant aspect is the two-sidedness of paper, *i.e.*, the difference in surface structure between the wire side and the top side. In filled papers, the felt side generally appears smoother (Naujock and Blechschmidt 2021) whereas filler-free laboratory papers often exhibit the opposite characteristic. The wire side, due to pure filtration on the forming wire, shows a more uniform, fine-grained structure, while the top side develops a coarser topography as a result of fiber accumulations (Bos *et al.* 2006). In addition, a filler gradient often develops across the thickness (Maren Freese 2010). Thus, even when the roughness distribution is reversed, the fundamental asymmetry between the two sheet surfaces remains.

This asymmetric surface structure affects not only optical or tactile properties but can also influence the mechanical adhesion conditions. The surface characteristics of paper, particularly in terms of roughness and porosity, play a decisive role in determining wetting, adhesion, and transfer behavior of liquids. Smoother, more conformable surfaces promote more uniform ink distribution and lead to sharper print quality (Kent and Parker 1973; Corson *et al.* 2004). These fundamental mechanisms can be transferred to ultrasonic welding, in which the bonding zone is often moistened, resulting in wetting processes comparable to those occurring in printing. Against this background, the hypothesis arises that the surface structure depending on the respective paper side can significantly influence the efficiency of energy transmission, the formation of the contact area, and the resulting joint strength in ultrasonic welding.

On a microscopic level, fiber length plays a decisive role in the mechanical strength of paper. Adequate fiber length promotes the formation of stable fiber–fiber bonds and supports effective stress distribution within the material (Horn 1974). In industrial manufacturing, however, fiber length is deliberately influenced through refining, *i.e.*, the mechanical treatment of the pulp, in order to optimize the mechanical properties of the final product particularly density, strength, and stiffness.

With increasing Schopper-Riegler value (SR), fiber treatment intensifies. In the present study, refining was carried out under laboratory-scale, low-intensity conditions to achieve defined SR values, primarily promoting fibrillation and fiber delamination, while also being associated with a progressive reduction in average fiber length at higher refining degrees. A recent study (Motamedian *et al.* 2019) indicates that fibrillation can make a significant contribution to the mechanical performance of paper. The improvements achieved through refining are primarily based on an increase in bonding density and a larger contact area for intermolecular bonds, which enhance the quality of fiber–fiber interconnections (Forsström *et al.* 2005; Borodulina *et al.* 2018). At the same time,

however, higher SR values also shorten fiber length, which can impair the ability to transfer stress macroscopically within the network. Less refined fibers, by contrast, retain greater length stability but exhibit lower surface activity, resulting in reduced cohesion in the bonding or joint area.

In light of these microstructural relationships, it can be hypothesized that the improvements in sheet strength achieved through refining may also have a positive influence on joint strength in ultrasonic bonding. Since in this process the joint is formed through local friction, thermal effects, and microscopic deformations, a high degree of fibrillation could potentially be advantageous for the formation of durable fiber–fiber connections within the joint zone.

Considering these complex interrelationships, the present study aimed to systematically investigate the influence of macroscopic structural features (fiber orientation, sheet side) as well as microscopic fiber parameters (fiber length and refining degree). The analysis focused on how these factorsindividually and in combination—affect joint strength and bonding quality in the ultrasonic bonding of paper.

EXPERIMENTAL

Materials and Measurements

The experiments were conducted under controlled climatic conditions at a temperature of 23 ± 1 °C. This study systematically investigated the influence of macroscopic and microscopic structural parameters on the ultrasonic bonding process and the resulting joint strength. To ensure a known and defined material composition, the materials used for the experiments were supplied by the Research and Service Institute for the Paper and Pulp Industry, the Papiertechnische Stiftung (PTS) in Heidenau, Germany. The selection of test materials enabled a systematic investigation of the influence of three key structural parameters: fiber orientation, sheet side (wire *vs.* top side, Fig. 1), refining degree (°SR value), on the quality of the bonded joint.

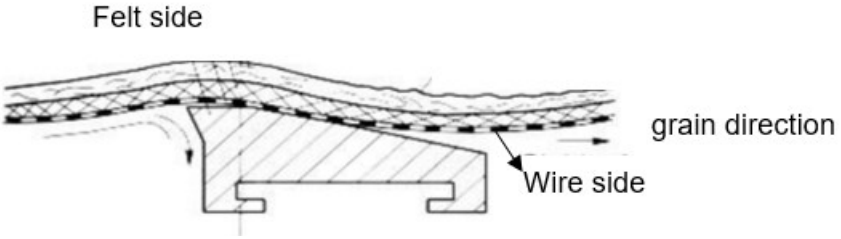

Fig. 1. Top side and wire side in the papermaking process. Note that the vertical deflection of the forming fabric is exaggerated in this schematic drawing.

An overview of the investigated papers and their respective properties is provided in Table 1. Since the substrates used are non-commercial trial papers, their identification is based on internal labeling (M1 to M9). All paper samples were uncoated. Apart from starch (HiCat 35844, Cargill, 1 %) and alkyl ketene dimer (AKD; Aquapel F220, Solenis, 0.7 %), no additional additives were used during production. The pulps used were produced using the kraft process, the most widely applied chemical pulping method worldwide.

For the experimental investigations, a total of nine different pulp-based papers were used, differing in fiber type, refining degree (°SR value), fiber length, and basis weight

(see Table 1). The basis weights of the materials were determined in accordance with ISO 536 (2020). Samples M1 to M7 were based on softwood (a mixture of spruce and pine, Stendal ECF) and thus contain long, flexible fibers that exhibit high tensile strength, whereas M8 and M9 were made from hardwood, specifically eucalyptus (UPM Eucalyptus), which contains shorter, stiffer fibers.

Table 1. Test Materials and their Properties

ID	Fiber Type	°SR Value	Grammage (g/m²)		Fiber Length (mm)	Thickness (µm)	Density (g/cm³)
			real	rounded			
M1	Spruce/Pine	24	79	80	1.82	135	0.59
M2	Spruce/Pine	24	122	120	1.82	192	0.63
M3	Spruce/Pine	24	176	170	1.82	267	0.66
M4	Spruce/Pine	36	81	80	1.65	125	0.65
M5	Spruce/Pine	36	121	120	1.65	177	0.68
M6	Spruce/Pine	80	80	80	1.17	118	0.68
M7	Spruce/Pine	80	130	120	1.17	181	0.720
M8	Eucalyptus	23	80	80	0.92	140	0.57
M9	Eucalyptus	23	169	170	0.92	270	0.61

Samples M1, M2, and M3 were based on spruce/pine pulp with a constant SR value of 24 and varying basis weights of 80, 120, and 175 g/m², respectively. The mean fiber length of these three samples was 1.82 mm. Samples M4 and M5 have an increased refining degree with an SR value of 36 and an average fiber length of 1.65 mm, with M4 having a basis weight of 80 g/m² and M5 of 120 g/m². Samples M6 and M7 represent the highest refining degree in the softwood series, with an SR value of 80. They differed in basis weight—80 g/m² for M6 and 120 g/m² for M7—but both exhibited a markedly reduced fiber length of 1.17 mm.

The two eucalyptus-based samples, M8 and M9, each had an SR value of 23 and an identical fiber length of 0.92 mm, but they differed in basis weight (80 and 170 g/m², respectively). This diversity of materials enables a differentiated analysis of the effects of fiber type, refining degree, basis weight, and fiber length on bonding properties

For improved comparability, the measured grammages of all paper materials listed in Table 1 were assigned to representative rounded grammage classes (80, 120, and 175 g/m²). The maximum deviation between the measured and rounded grammage occurred in the 120 g/m² class and was less than 8% (*e.g.*, 130 g/m² assigned to 120 g/m²: approx. 7.7%). The density calculation, however, was performed using the actual measured grammage and the corresponding thickness.

For the systematic analysis of the influence of fiber orientation on joint strength in ultrasonic bonding, materials M1, M3, M8, and M9 were used. Sample preparation was carried out in both the machine direction (MD) and the cross direction (CD), so that the resulting joints were either perpendicular or parallel to the fiber orientation (Fig. 2).

The aim of this investigation was to identify potential relationships between fiber orientation and local fiber displacements or structural inhomogeneities during the bonding process, as well as to quantitatively evaluate their effects on the resulting joint strength. The selection of materials M1, M3, M8, and M9 enabled a comparison between two different fiber types—softwood fibers (spruce/pine) and hardwood fibers (eucalyptus)—

and two different basis weights (80 and 170 g/m²). This differentiation made it possible to consider not only the influence of fiber orientation but also structural parameters such as fiber type and basis weight. The bonding parameters were kept constant in all experiments: amplitude 85 % (25.5 µm), and a joining force of 1400 N, which corresponds to a process pressure of approximately 18.5 MPa on the weld area of 5 × 15 mm, with bonding energy 10 J. Prior to bonding, all samples were moistened with 3 µL of water to ensure defined initial conditions.

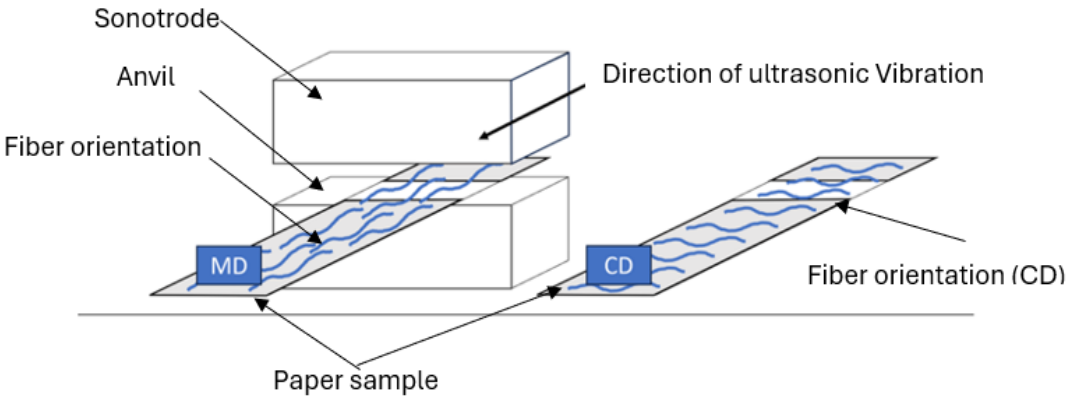

Fig. 2. Schematic representation of fiber orientation in the ultrasonic bonding process

To investigate the influence of the paper side on the bonding properties, the same materials as in the previous experiments (M1, M3, M8, and M9) were used. The samples were deliberately positioned so that either the wire side or the top side was located in the bonding zone. This targeted placement enabled a differentiated analysis of the effects of paper side on the bonding process. The test series was carried out while varying the fiber type (softwood: spruce/pine *vs.* hardwood: eucalyptus) and the basis weight (80 or 170 g/m²) in order to rule out potential interactions between paper side, fiber type, and basis weight, and to isolate the effect of paper side. The results of the mechanical tests were then comparatively evaluated.

To assess the influence of fiber refining on the mechanical properties of ultrasonic weld joints, a total of six paper materials were used, differing in two basis weights (80 g/m² and 120 g/m²) and three defined refining levels each. The samples with a basis weight of 80 g/m² included M1 (°SR 24), M4 (°SR 36), and M6 (°SR 80). The samples with a basis weight of 120 g/m² included M2 (°SR 24), M5 (°SR 36), and M7 (°SR 80). While °SR 24 and °SR 36 values correspond to typical industrial applications, the exceptionally high refining level of SR 80 was specifically produced to examine the effects of intensive fiber refining on the bonding zone in more detail. The higher degree of fiber fineness and flexibility is intended to reveal potential correlations between the microstructure of the paper and the quality of the bonded joint. This material matrix enables a differentiated analysis of the interaction between fiber refining (refining intensity) and basis weight with regard to their effect on the mechanical integrity of the weld seam in the ultrasonic process.

An experimental plan comprising 20 different parameter combinations was developed (Table 2) to define a process window that enables reliable joining while achieving high joint strength and avoiding undesired effects such as local overheating or burning phenomena in the joint zone. In addition, the joining process was intended to be performed with the lowest possible bonding force and reduced energy input in order to

minimize mechanical wear of the ultrasonic welding equipment while maintaining a high process speed.

The minimum and maximum ultrasonic welding parameters were defined based on preliminary experiments. The selection of parameter combinations was carried out using the *Cornerstone* software, with low, medium, and high levels of energy input, bonding force, and amplitude being systematically varied. This approach enabled the investigation of process sensitivity as well as the identification of potential interaction effects between parameters and covers a process window that is relevant both for fundamental understanding of the joining process and for potential industrial application. To ensure comparability, the same experimental design was applied to all investigated paper materials

Each of these combinations was applied identically to all samples with varying °SR values. To ensure the reliability of the results, each experiment was repeated five times, and the mean values were calculated. This ensured that the experimental conditions were kept constant across all samples, allowing any observed differences in the resulting joint strength to be attributed solely to the respective SR value rather than to variations in the welding parameters.

Table 2. Welding Parameters

Amp (%)	Force	Energy (J)	Moisture. (µL)
70	400	10	0
70	1400	10	0
100	1400	40	3
100	1400	10	0
70	400	40	0
70	400	10	3
100	400	10	0
100	400	10	3
70	400	40	3
85	1067	10	3
85	1400	40	0
100	1067	30	0
100	1400	10	3
100	400	30	3
100	400	40	0
85	733	40	3
70	1400	40	3
85	400	20	0
70	1067	40	0
70	1400	20	3

Using a cutting device, test strips with a width of 15 mm were cut from the paper sheets, ensuring a clamping length of 50 mm. To minimize potential influences from different fiber orientations, all specimens were taken longitudinally in the machine direction (MD) of the paper. The area to be moistened, which simultaneously serves as the welding zone, was then marked on the specimens. This welding zone measured 5 mm × 15 mm and was positioned on the top side of the paper. The side facing away from the wire at a defined distance of 5 mm from the upper edge of the specimen. On the wire side, *i.e.*, the side facing the forming wire an additional mark was made at a distance of 10 mm from the upper edge to ensure precise and reproducible positioning of the specimens between the sonotrode and the anvil during the welding process.

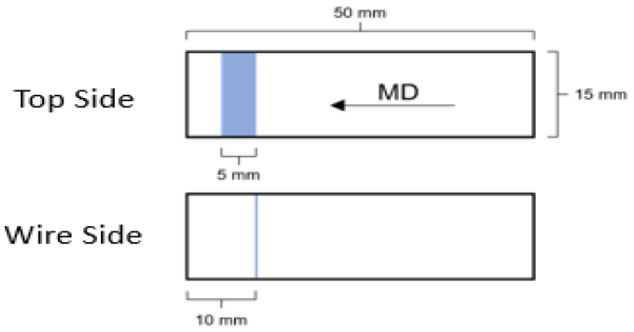

Fig. 3. Schematic representation of specimen preparation and marking of the welding area

In test series specifically investigating the influence of the wire side, the alignment was reversed accordingly. In such cases, the welding zone was located on the wire side, and the distances from the upper edge were mirrored. A schematic representation of the sample preparation is shown in Fig. 3.

Test Equipment and Devices Used

To investigate the influence of macroscopic and microscopic structural parameters on the weld zone in ultrasonic bonding, targeted experimental series were conducted on an ultrasonic test bench provided by Herrmann Ultraschalltechnik (Fig. 4). Macroscopic and microscopic parameters such as fiber orientation, paper surface (wire side *vs.* felt side), and fiber length were systematically varied to analyze their impact on the quality of the bonded joint.

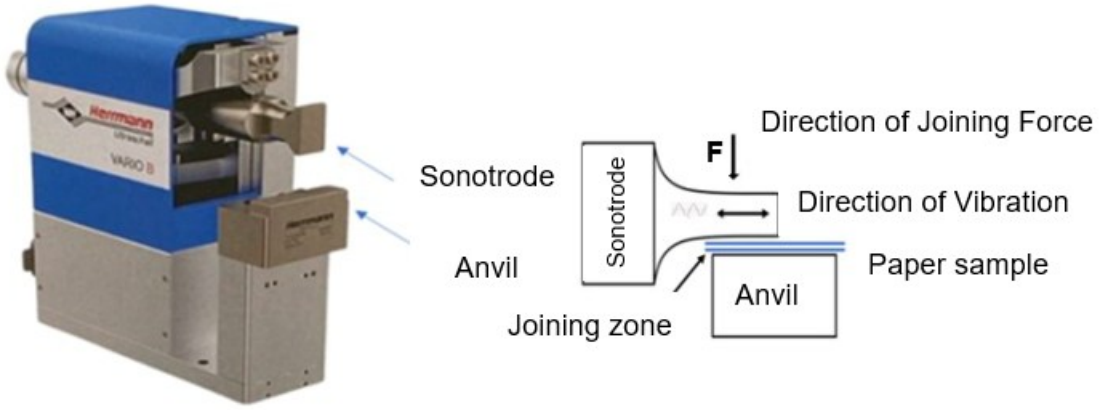

Fig. 4. Basic configuration of the ultrasonic test stand

The test stand generates ultrasonic vibrations with a nominal frequency of 20 kHz and a maximum vibration amplitude of 31.9 µm. Four sonotrode surface contours and two anvil surface contours can be used interchangeably. A finely textured waffle sonotrode surface measuring 1.0 × 0.4 mm was applied to the surface at an angle of 45°, together with a waffle-textured anvil surface measuring 0.5 × 0.175 mm, also at an angle of 45° (Fig. 5).

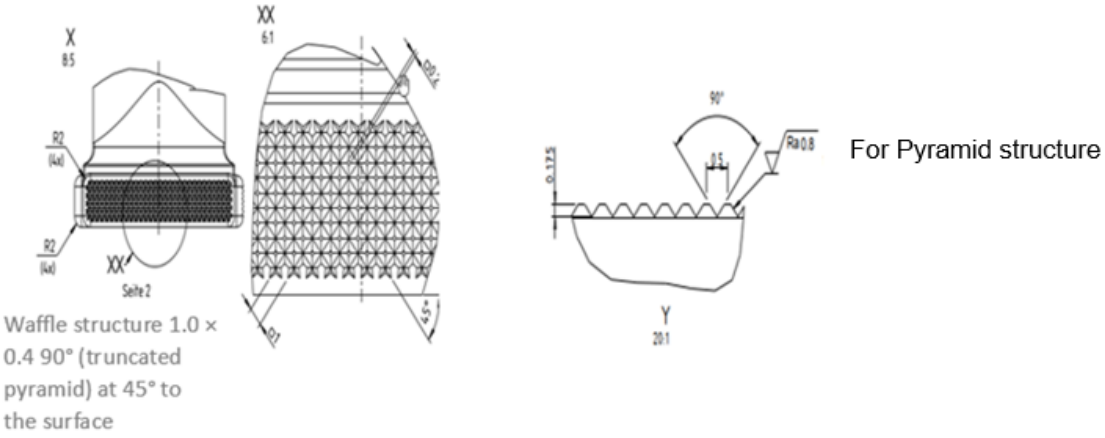

Fig. 5. Waffle sonotrode surface on the left, waffle anvil surface on the right. (Herrmann Ultraschalltechnik GmbH & Co.)

Immediately before joining the samples, one of the two sample strips was moistened in the defined area. Unless otherwise specified in the test description, 3 µL of demineralized water was applied using a piston-operated pipette. The applied water was then distributed evenly over the entire marked area using a glass rod, avoiding the application of pressure. The second sample strip was placed flush on the moistened sample strip without moistening. When joining without moistening, the two upper sides of the paper strips were placed directly on top of each other without further pre-treatment. The samples were then placed in the ultrasonic welding device so that the mark on the outside (screen side) was aligned with the outer edge of the sonotrode. This ensures that the full surface of the joining tools acts on the moistened joining surface.

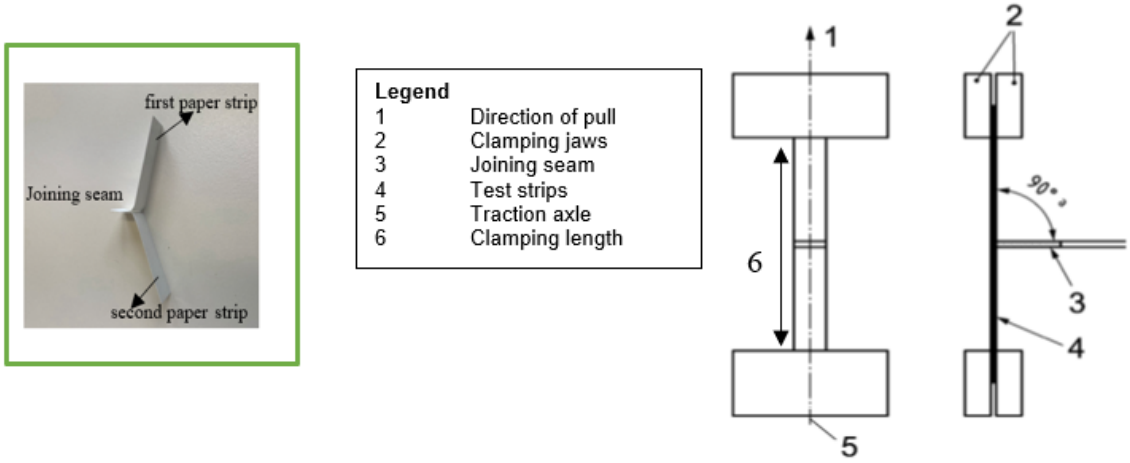

Fig. 6. Schematic diagram of the test arrangement according to DIN 55529 (2012)

Once the samples had been positioned correctly between the anvil and sonotrode, the joining process could be started. The sonotrode moved towards the anvil with a defined force. As soon as the trigger point was reached, ultrasonic vibrations were introduced into the joining partners, which continued until the pre-defined amount of energy was reached.

After completion of the joining process, the samples were acclimatized for at least two hours in a standard climate at a temperature of 23±1 °C to ensure defined drying before the joint strength was determined.

To evaluate the joint strength, a peel test was carried out in accordance with DIN 55529 (2012). The tests were performed using a testing machine from the manufacturer ZwickRoell GmbH & Co. KG (model Xforce HP 1 kN, Z016 with BT1-FR010TM.A50). The joined paper strips were clamped in a tensile testing machine so that they were positioned perpendicular to the tensile direction, and a peel angle of 90° was created. The samples were clamped in the center of the tensile axis with a free clamping length of 50 mm. (Fig. 6). The pull-off speed was a constant at 100 mm/min during the measuring process. The test took place in a standardized climate chamber.

A force-displacement diagram was recorded for each measurement process, from which the maximum force (F_{max}) can be taken. The average value of the maximum forces is calculated from a series of five test samples. This describes the joint strength of a series of samples. The factors and parameters investigated in this study are systematically presented in Table 3. For each factor and parameter, it is also indicated whether it is a continuous or a categorical variable. Continuous factors are quantitative and have a fixed order, whereas categorical factors represent qualitative data without a natural order.

Table 3. Overview of the Factors and Parameters Analyzed

Factor	Unit	Variable type
Fiber Orientation	MD/CD	Categorical
Paper Side	Top / Wire Side	Categorical
Refining Degree (SR Value)		Categorical
Material Type		Categorical

RESULTS AND DISCUSSION

The analysis of the experimental data shows that joint strength was influenced by several interacting parameters, including fiber orientation, paper side, basis weight, fiber type, and refining degree. Among these parameters, fiber orientation exhibited the strongest and most consistent effect on the mechanical performance of the joints. Paper side and refining degree also affected joint strength, although their impact strongly depended on the material combination and processing conditions. Overall, it becomes clear that the mechanical properties of the joint were determined by a complex interplay of structural and surface-related factors. In the following sections, the individual effects of fiber orientation, paper side, and refining degree are analyzed and discussed in detail.

The results shown in Fig. 7 of the experimental series demonstrate that fiber orientation had a significant influence on joint strength. In all investigated material combinations, both for spruce/pine and eucalyptus, as well as for both tested grammages (80 and 170 g/m²), Samples cut in the machine direction (MD), in which the fiber orientation during the joining process coincides with the vibration direction, exhibited higher joint strengths than samples cut in the cross direction (CD), where the vibration direction is oriented perpendicular to the fiber orientation. The smallest difference between MD and CD was observed for spruce/pine with 80 g/m², where joint strength increased from 4.61 N (CD) to 4.93 N (MD), a gain of +0.32 N. The largest difference appeared for eucalyptus with 80 g/m², increasing from 3.48 N (CD) to 5.15 N (MD), a difference of +1.67 N. A similar trend was observed at 170 g/m²: for spruce/pine, strength rose from 2.57 N (CD) to 3.58 N (MD) (+1.01 N), and for eucalyptus from 2.50 N to 3.53 N (+1.03 N).

Although paper fundamentally differs from fiber-reinforced thermoplastics in that it contains no polymer matrix and the fibers are bonded directly to each other rather than being embedded in a continuous resin phase, the observed influence of fiber orientation on joint strength shows a remarkable similarity. In this respect, the present results are consistent with the findings reported by (Köhler *et al.* 2021)**.** for fiber-reinforced thermoplastic systems, where fiber alignment along the load or joining direction likewise led to enhanced mechanical performance.

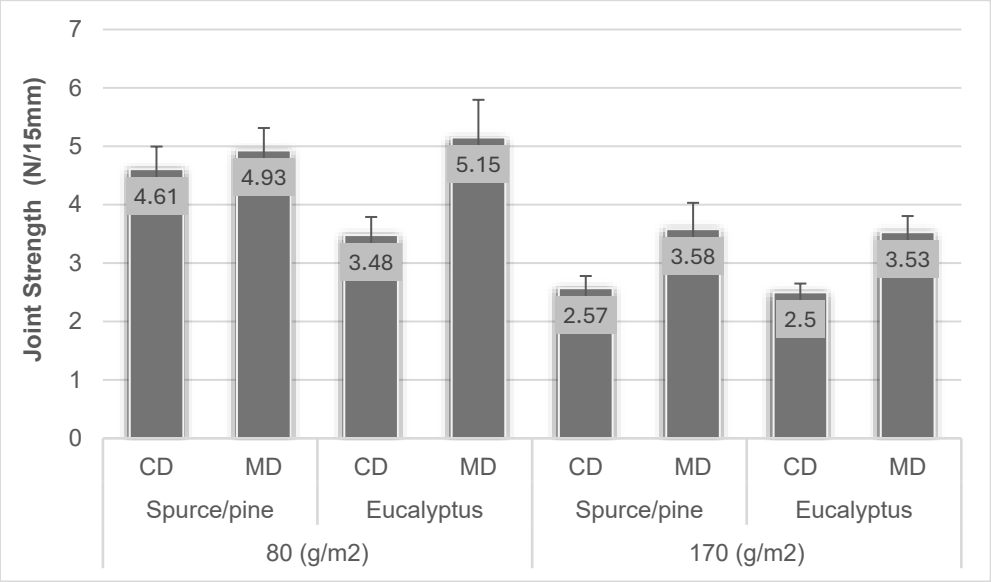

Fig. 7. Influence of fiber orientation on joint strength

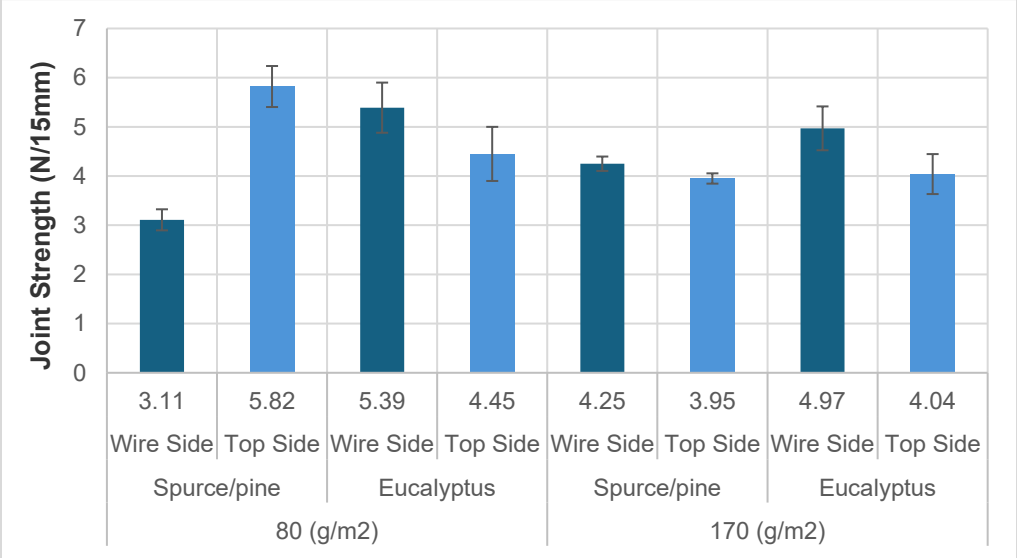

Fig. 8. Influence of wire side and top side on the joint strength

This consistently higher strength for MD samples indicates that fiber orientation aligned with the joining direction positively affected the mechanical load-bearing capacity of the joint. The results suggest that fiber orientation should be taken into account when aligning joining partners during the process to achieve maximum joint strength.

The measured joint strengths (in N/15 mm) shown in Fig. 8 reveal clear differences between the wire side and the top side depending on fiber type and basis weight. At the lower basis weight of 80 g/m², the spruce/pine paper achieved a significantly higher strength on the top side with 5.82 N compared to the wire side (3.11 N). Conversely, the eucalyptus paper at the same basis weight showed higher joint strength on the wire side (5.39 N) compared to the top side (4.45 N). At the higher basis weight of 170 g/m², the differences diminished. For spruce/pine, the wire side slightly outperformed the top side (4.25 *vs.* 3.95 N), while eucalyptus again showed higher strength on the wire side (4.97 N) compared to the top side (4.04 N).

These results demonstrate that the paper side did influence joint strength. However, this influence was not consistent but depended on the fiber type and basis weight used. Different combinations exhibit opposing trends, indicating that the effects of the paper side are superimposed by other parameters such as fiber structure, porosity, or surface roughness. Due to these complex interactions, no general, linear relationship between paper side and joint strength could be established. Therefore, no universal advantage of the wire side or the top side can be assumed.

Table 4. Experimental Plan for Investigating the Influence of the °SR Value on the Resulting Weld Joint Strength

		Grammage (g/m²)			80			120		
					80	80	80	130	120	120
		ID			**M6**	**M4**	**M1**	**M7**	**M5**	**M2**
		SR Value			**80**	**36**	**24**	**80**	**36**	**24**
V-Nr.	Amp (%)	Force (N)	Energy (J)	Moisture (µl)	**Joint Strength (N/ 15 mm)**					
1	70	400	10	0	0.9	1.00	1.9	0.3	0.80	0.9
2	70	1400	10	0	2.6	2.79	3.1	4.1	1.79	2.9
3	100	1400	40	3	2.5	4.14	5	5.4	6.49	5.3
4	100	1400	10	0	3.2	2.25	4.2	3.7	1.90	3.3
5	70	400	40	0	1.5	1.57	2	1.2	3.79	3.2
6	70	400	10	3	3	2.67	3	4.3	2.96	3.5
7	100	400	10	0	0.9	1.34	2.4	0.6	0.80	1.6
8	100	400	10	3	2.8	2.10	2.6	4	2.67	2.7
9	70	400	40	3	1.1	1.46	2.4	2.7	0.55	2.4
10	85	1067	10	3	4	3.19	5.4	6.1	3.57	4
11	85	1400	40	0	3.4	2.36	2.9	7.2	6.30	4.6
12	100	1067	30	0	1.6	2.47	2.9	7.3	5.99	4.1
13	100	1400	10	3	3.6	3.25	5.4	5.6	4.48	4.3
14	100	400	30	3	1.3	1.31	2.7	3.4	2.19	1.9
15	100	400	40	0	1	3.52	1.8	5.6	2.76	4.1
16	85	733	40	3	1.4	2.63	2.8	6	3.87	4.2
17	70	1400	40	3	2.5	3.55	4.9	6.8	6.09	5.9
18	85	400	20	0	0.6	2.06	2.6	1	2.08	3.6
19	70	1067	40	0	1.7	2.92	2.9	7	4.59	4.7
20	70	1400	20	3	3.4	4.15	5.8	7.7	4.52	6.1
				SR Value ⌀	**2.1**	**2.5**	**3.3**	**4.5**	**3.4**	**3.7**

The investigations carried out on the influence of refining degree on joint strength revealed significant differences in the mechanical properties of the bonding zone depending on the Schopper–Riegler value (°SR) of the papers used. An overview of the determined joint strengths is presented in Table (4). For improved comparability, the

highest strength values for each material are highlighted in green, and the lowest values are highlighted in red. The mean values across all test series for each material are summarized in the last row.

With low basis weight, the highest seam strength was observed at a low degree of refining (°SR 24), whereas a high degree of refining (°SR 80) led to reduced strength. The lowest investigated refining level (°SR 24) produced the highest seam strength values in 16 out of 20 test series and achieved the second-highest values in the remaining four cases. Notably, °SR 24 did not yield the lowest strength in any of the experiments. In contrast, the highest refining level (°SR 80) was associated with the lowest measured weld seam strength in 13 out of 20 cases. Only in two test series did this high refining level achieve the top value. This distribution indicates a systematic impairment of strength properties in highly refined pulp for papers with low basis weight. The average strength loss from °SR 24 to °SR 36 was 0.8 N, while a further increase to °SR 80 results in an additional reduction of only 0.4 N.

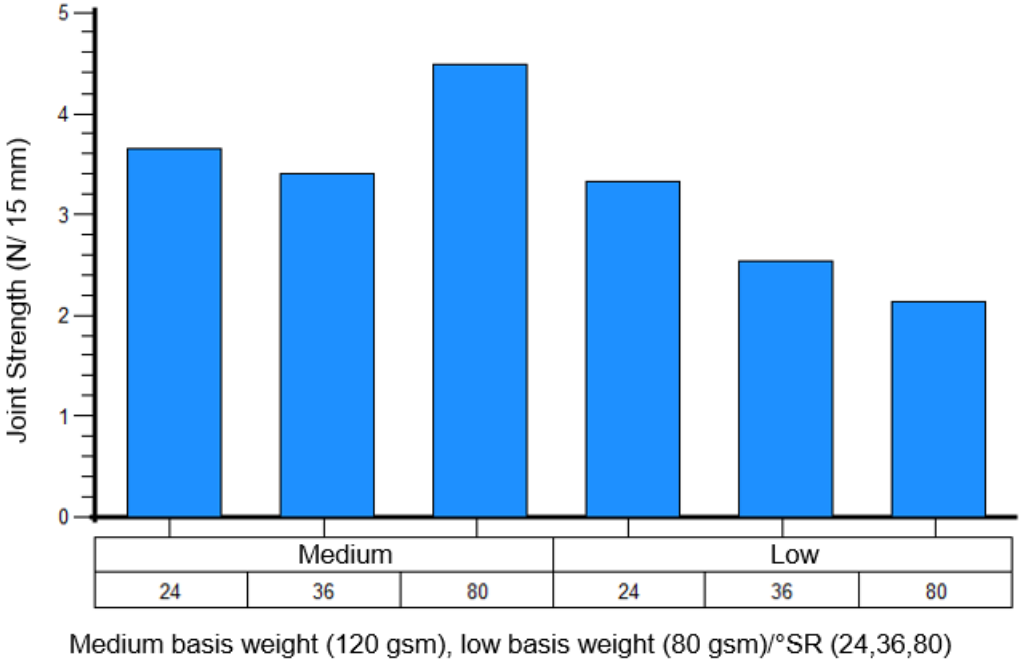

Fig. 9. Influence of SR-Value on joint strength

In contrast, papers with higher basis weight exhibited the opposite trend. The results show that a high degree of refining (SR 80) generally led to the highest weld seam strengths. In 15 out of 20 analyzed cases, SR 80 produced the maximum strength value within the respective test series. The mean seam strength at this refining level was 4.5 N/15 mm, clearly exceeding the mean values of °SR 36 (3.4 N/15 mm) and °SR 24 (3.7 N/15 mm). Notably, the lowest refining level (°SR 24) yielded slightly higher average strength values than the medium refining level (°SR 36), although the difference of 0.3 N/15 mm was small and was within the experimental scatter. These observations suggest that, in the range of low to medium refining levels (°SR 24 to SR 36), no clear correlation between refining level and seam strength was established. Only at a substantially increased refining level (°SR 80) did a consistent positive effect on the mechanical strength of the weld zone become apparent.

To improve clarity and enable direct comparison of the contrasting trends at low and medium basis weights, the mean seam strengths are summarized in Fig. 9 as a function of refining degree. Figure 9 highlights the strong basis-weight-dependent influence of refining degree on seam strength. While a continuous decrease in mean seam strength is observed with increasing refining degree at low basis weight (80 g/m²), an opposite trend is evident at medium basis weight (120 g/m²), with maximum strength values occurring at a high refining level (SR 80). The figure therefore provides a compact summary of the key trends derived from the comprehensive results table.

To quantitatively support the observed trends, a multiple linear regression analysis was performed (see Tabel 5). The model explains a substantial portion of the variance in joint strength ($R^2 = 0.82$, adjusted $R^2 = 0.76$). Among the investigated parameters, the interaction between grammage and refining degree (SR) shows the highest statistical significance ($p < 0.01$), while grammage and refining degree alone do not exhibit significant main effects. This indicates that surface-related effects become relevant primarily through parameter interactions rather than as isolated factors.

Table 5. Regression Model: Effects and Interactions of Process Parameters on Joint Strength

Term	P-Value	Term	P-Value
Constant	0.8	Energy × SR	0.104
Refining degree (SR)	0.288	Moistening × SR	0.447
Basis weight	0.089	Amplitude×Basis weight	0.512
Amplitude	0.887	Basis weight × Force	0.006
Force	0.019	Energy × Basis weight	2e−07
Energy	0.48	Moistening×Basis weight	0.829
Moistening	2e−04	Amplitude × Force	0.439
Basis weight×SR	2e−06	Amplitude × Energy	0.103
Moistening ×SR	0.477	Amplitude ×Moistening	0.019
Force×SR	0.373	Energy × Force	0.133
Moistening × Energy	9e−08	Moistening × Force	0.105
R-Square	0.818	Adj-R-Square	0.757
RMS-Error	0.839	Residual df	89

This observation can be explained by the shortening of fibers at advanced refining levels. In thinner papers with low basis weight, the fiber network is overall less compact and mechanically less consolidated. As described in the literature (Seth and Page 1988), under such conditions fiber length is a dominant factor for tear strength and, by extension, for seam strength, since longer fibers might enable more bonding along their axis and thus more effective force transfer within the network. Fiber shortening caused by refining has a negative effect in this case, as the advantages of fibrillation seem to be overcompensated by the reduction in fiber length.

In contrast, the opposite dependence between refining degree and seam strength observed for papers with medium basis weight can be attributed to the dominant effect of intense fibrillation at high refining levels. The mechanical action during refining splits the fiber surfaces into extremely fine fibrils, thereby significantly increasing the specific surface area. This might promote the formation of numerous contact points between fibers, particularly through intermolecular hydrogen bonding. Due to the high density of hydroxyl groups in cellulose, close fiber–fiber contact enables the formation of stable hydrogen bonds, which contribute substantially to cohesion and, consequently, to the strength of the joint.

The microscopic investigations provided qualitative indications that were consistent with the structural changes (Fig. 10). Material A with a low °SR value (°SR 26) was characterized by predominantly long fibers with an average fiber length of approximately 1.82 mm, while only minor indications of fiber shortening were observed. The fiber arrangement appeared relatively open and loosely packed, with an inhomogeneous surface distribution, which was reflected by pronounced bright and dark regions in the micrographs. In contrast, Material B with a high refining degree (°SR 80) exhibited predominantly shorter fibers with an average fiber length of approximately 1.17 mm, indicating a reduced fiber length and possible fiber fragmentation at high refining levels. The surface appeared more densely packed and homogeneous overall, while bright regions, which may be interpreted as qualitative indicators of pores or uncovered zones, are markedly reduced. Overall, the observed fiber arrangements suggest a more uniform and compact surface structure at high refining degrees

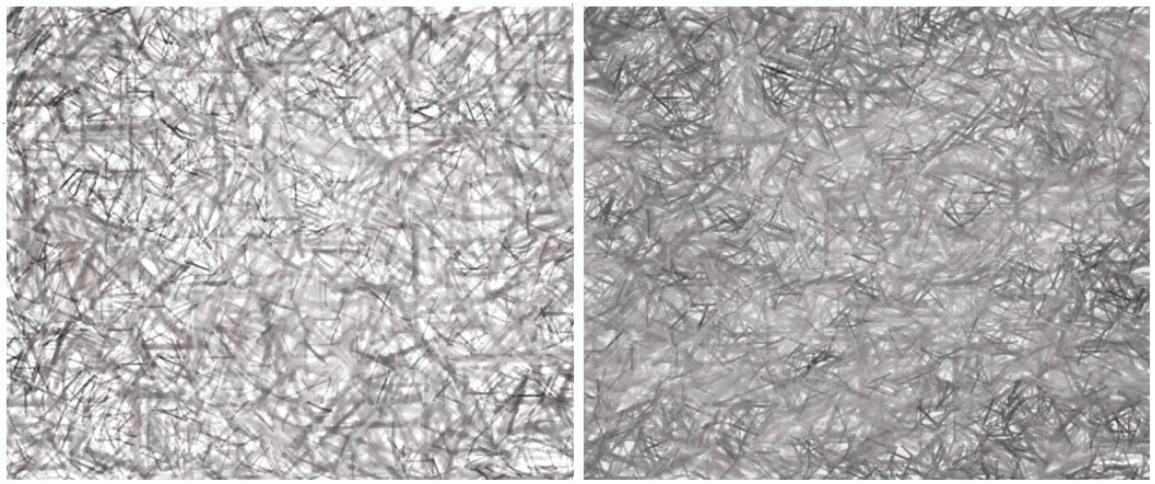

Fig. 10. Brightfield microscopy images of the fiber surface: Left M1 (SR=24) *vs.* right M6 (SR 80)

The results overall demonstrate that the influence of refining degree (°SR) on joint strength was clearly dependent on the basis weight. For high basis weight papers (*e.g.*, 160 g/m²), the positive effect of fibrillation predominated, as the increased specific surface area and bonding density led to improved joint strength. In contrast, for low basis weight papers (80 g/m²), the negative impact of shortened fibers and reduced contact points dominates, causing joint strength to decrease at high refining degrees.

CONCLUSIONS

1. A key finding concerns fiber orientation. Across all investigated materials, independent of fiber type and basis weight, joined samples with fibers aligned parallel to the vibration direction exhibited higher joint strengths than samples with fibers oriented transversely. From a practical perspective, it therefore appears advisable, where feasible, to prefer a joining orientation in industrial packaging layouts in which the vibration direction and the fiber orientation are aligned parallel to each other, in order to achieve higher joint strength. From a practical perspective, it is therefore advisable, where feasible, to prefer, as this results in higher joint strengths.
2. The paper side (wire side *vs.* top side) was also identified as a relevant influencing factor, with its effect being strongly dependent on fiber type and basis weight. The observed differences indicate complex interactions between paper side, surface characteristics, and internal fiber structure, such that no clear linear relationship can be established. Consequently, a general advantage of either paper side cannot be derived.
3. The results further indicate that the refining degree (°SR) had a significant, yet strongly basis-weight-dependent influence on the mechanical integrity of the joint. For papers with high basis weight (*e.g.*, 170 g/m²), higher refining levels (approximately °SR 80) were associated with increased joint strength, as intensive fibrillation promotes the formation of dense fiber networks and enhanced bonding within the joint zone. In contrast, for papers with low basis weight (80 g/m²), lower refining levels (approximately °SR 24) were more favorable, since increased internal bonding within the paper structure at high refining levels limits the availability of free fiber surfaces for inter-sheet bonding and thus constrains joint strength. Changes in fiber length associated with intensive refining may further modulate this behavior.

Overall, the findings suggest that the deliberate adjustment of refining degree and the selection of joining direction represent effective parameters for influencing joint strength. Other factors, such as the paper side, exhibit more complex and context-dependent effects and therefore require a differentiated evaluation during process design.

REFERENCES CITED

Alava, M., and Niskanen, K. (2006). "The physics of paper," *Reports on Progress in Physics* 69(3), 669-723. https://doi.org.10.1088/0034-4885/69/3/r03

Borodulina, S., Motamedian, H. R., and Kulachenko, A. (2018). "Effect of fiber and bond strength variations on the tensile stiffness and strength of fiber networks," *International Journal of Solids and Structures* 154, 19-32. https://doi.org.10.1016/j.ijsolstr.2016.12.013

Bos, J. H., Staberock, M., and Bos, J. H. (eds.). (2006). *Das Papierbuch: Handbuch der Papierherstellung*, ECA Pulp & Paper b.v, Houten, Netherlands.

Corson, S. R., Flowers, A. G., Morgan, D., and Richardson, J. D. (2004). "Paper structure and printability as controlled by the fibrous elements," *TAPPI Journal* 3(6), 14-18.

DIN 55529 (2012). "Packaging – Determining the sealed-seam strength of sealings made of flexible packaging material," Deutsches Institut für Normung e.V., Berlin, Germany.

ISO 536 (2020). "Paper and board - Determination of grammage," International Organization for Standardization, Geneva, Switzerland.

Forsström, J., Andreasson, B., and Wågberg, L. (2005). "Influence of pore structure and water retaining ability of fibres on the strength of papers from unbleached kraft fibres," *Nordic Pulp & Paper Research Journal* 20(2), 176-185. https://doi.org.10.3183/npprj-2005-20-02-p176-185

Horn, R. A. (1974). *Morphology of Wood Pulp Fiber from Softwoods and Influence (Research Paper FPL 242)*, U.S. Department of Agriculture, Forest Products Laboratory, Madison, WI, USA. https://www.fpl.fs.usda.gov/documnts/fplrp/fplrp242.pdf

Köhler, F., Villegas, I., Dransfeld, C., and Herrmann, A. (2021). "Static ultrasonic welding of carbon fibre unidirectional thermoplastic materials and the influence of heat generation and heat transfer," *Journal of Composite Materials* 55(15), 2087–2102. https://doi.org.10.1177/0021998320976818

Freese, M. (2010). *Einfluss verschiedener Bleichfolgen auf die Hemicellulosen-zusammensetzung und -verteilung über den Querschnitt der Faserwand*, Ph.D. Dissertation TU Dresden, Germany.

Motamedian, H. R., Halilovic, A. E., and Kulachenko, A. (2019). "Mechanisms of strength and stiffness improvement of paper after PFI refining with a focus on the effect of fines," *Cellulose* 26(6), 4099-4124. https://doi.org.10.1007/s10570-019-02349-5

Naujock, H.-J., and Blechschmidt, J. (eds.). (2021). *Taschenbuch der Papiertechnik*, Hanser, München, Germany.

Kent and Parker, J. R. (1973). "Fundamental paper properties in relation to printability," in: *Transactions of the Vth Fundamental Research Symposium*, F. Bolam (ed.), Fundamental Research Committee (FRC), Manchester, UK, pp. 517-543. https://doi.org.10.15376/frc.1973.2.517

Seth, R. S., and Page, D. H. (1988). "Fiber properties and tearing resistance," *TAPPI Journal* 71, 103.

Article submitted: October 7, 2025; Peer review completed: December 13, 2025; Revised version received: January 13, 2026; Accepted: February 17, 2026; Published: February 27, 2026.
DOI: 10.15376/biores.21.2.3593-3608